SPATIAL PREDICTION OF NONLINEAR RANDOM OCEAN WAVES: IDENTIFICATION OF GAUSSIAN AND NON-GAUSSIAN CONTRIBUTIONS

Steven R. Winterstein, Bert Sweetman
Dept. of Civil and Environmental Eng., Stanford University, Stanford, CA 94305-4020
steve@ce.stanford.edu, sweetman@stanford.edu

Alok K. Jha
Risk Management Solutions, Menlo Park, CA 94025
alokj@riskinc.com

Abstract

Statistical properties and simulation methods for non-Gaussian (second-order random) ocean waves are reviewed here. A new method is introduced to address the "inverse" problem: if an observed wave history results from second-order random theory, how can separate Gaussian and non-Gaussian contributions be identified? The value of this identification method is demonstrated in cases where wave histories must be extrapolated spatially—e.g., for spatially distributed ocean structures and ships. The standard linear dispersion approach, while consistent with second-order theory, is shown to produce unstable spatial wave statistics, producing more nearly Gaussian behavior after spatial extrapolation. In contrast, the identification method proposed here permits "selective linear dispersion," applied only to the identified Gaussian part of the total wave process. This selective linear dispersion is found to yield spatially stable non-Gaussian models, accurately preserving the theoretical statistics of second-order random waves.

Introduction and Background

Analysis and design of ocean structures require an accurate model of the time-varying wave surface elevtion, $x(t)$, at one or more spatial locations. The simplest such model is provided by a Gaussian process, which arises as a result of first-order, linear wave theory. We denote this first-order model as $x_1(t)$, written as a Fourier sum as

$$x_1(t) = \sum_{k=1}^{N/2} A_k \cos(\omega_k t + \theta_k) = \sum_{k=1}^{N} X_{1,k} \mathrm{e}^{i\omega_k t} \tag{1}$$

where X_k=$A_k \exp(\mathrm{i}\theta_k)/2$ for $k \leq N/2$, and X_{N-k} is the complex conjugate of X_k. The amplitudes A_k=$\sqrt{2S(\omega_k)\Delta\omega}$ preserve an arbitrary (one-sided) wave spectrum $S(\omega)$ at the discrete frequencies ω_k, while the mutually independent phases θ_k are generated from identical uniform distributions between 0 and 2π.

Beyond its obvious simplicity, the Gaussian model has the advantage of spatial stability: because the spatial evolution of waves is commonly predicted by linear dispersion theory, the Gaussian nature of $x(t)$ will be preserved by this linear operation. The Gaussian model, however, fails to preserve nonlinear effects, such as the marked asymmetry shown by ocean

waves: wave crests that systematically exceed their neighboring troughs. This asymmetry increases with decreasing water depth, but remains present even in deep-water sites.

Viewing $x_1(t)$ as the solution to the linearized free surface condition, second-order perturbation suggests a modified wave history, $x(t)$=$x_1(t)$+$x_2(t)$, in which the second-order correction $x_2(t)$=$\sum_{k=1}^{N}[X_{2,k}^{+} + X_{2,k}^{-}]\exp(\mathrm{i}\omega_k t)$ includes the sum- and difference-frequency contributions

$$X_{2,k}^{+} = \sum_{m+n,k} X_{1,m}X_{1,n}H_{mn}^{+} = \sum_{m+n,k} \left[(U_m U_n - V_m V_n) + \mathrm{i}(V_m U_n + U_m V_n)\right] H_{mn}^{+} \quad (2)$$

$$X_{2,k}^{-} = \sum_{m-n,k} X_{1,m}X_{1,n}H_{mn}^{-} = \sum_{m-n,k} \left[(U_m U_n + V_m V_n) + \mathrm{i}(V_m U_n - U_m V_n)\right] H_{mn}^{-} \quad (3)$$

In these results, H_{mn}^{+} and H_{mn}^{-} are sum- and difference-frequency quadratic transfer functions (QTFs). These are analytically available for arbitrary water depths (e.g., Tick, 1959; Hasselmann, 1962). The sums here are intended to include all (m, n) pairs such that $1 \leq m, n \leq N/2$ and $m \pm n$=k ("+" for Eq. 2; "-" for Eq. 3). Finally, in the latter form of Eqs. 2–3, U_k=Re$(X_{1,k})$ and V_k=Im$(X_{1,k})$.

Numerical Results

Figure 1 shows the simulated time-varying behavior of both $x_1(t)$ and $x_2(t)$, and the resulting total wave process $x(t)$=$x_1(t)$+$x_2(t)$. We assume $x_1(t)$—and hence, to good approximation, $x(t)$—has a JONSWAP power spectrum, with significant wave height H_S=15.4m, peak spectral period T_P=17.8s, and peakedness factor γ=1.7. These parameters are roughly representative of 100-year conditions in the Northern North Sea, and have served as the basis for extensive wave tank tests in which "ringing" response of a tension leg platform was observed. This figure shows a selected episode, which includes the maximum of $x(t)$, during a T=3 hour simulation with dt=0.45s. The total simulation hence comprises N=24000 time points, and N^2=.576 $\times$ 10^9 double-frequency contributions to $x_2(t)$. Note that due to sum-frequency effects, $x_2(t)$ has significant frequency content near $2f_p$; i.e., twice the characteristic frequency f_p=1/T_p of $x_1(t)$. Also, as Figure 1 shows, $x_2(t)$ histories tend to be "phase locked" with $x_1(t)$: positive peaks of $x_2(t)$ tend to align with both peaks and troughs of $x_1(t)$. This results in a total process $x(t)$ that is notably skewed, in conformance with observed wave tank and ocean field behavior (e.g., Jha and Winterstein, 2000).

Figure 2 shows power spectra corresponding to the simulated histories in Figure 1. Most notably, $x_1(t)$ is shown to have far more power than $x_2(t)$ even at "high frequencies"; e.g., in the vicinity of $2f_p$. Hence, simple bandpass filtering of $x(t)$ will not accurately separate it into first- and second-order contributions. This separation instead requires careful analysis of the entire time history—or equivalently, of both its Fourier phases as well as its amplitudes. The history $x_2(t)$ should be assigned only to the (generally small) portion of the total power of $x(t)$ that is phase-locked with $x_1(t)$. Such an identification procedure to separate $x(t)$ into $x_1(t)$ and $x_2(t)$ is shown in the next section.

Identification and Selective Linear Dispersion

We now assume that an observed wave time history, $x_{obs}(t)$=$\sum_{k=1}^{N} X_{o,k} \exp(\mathrm{i}\omega_k t)$, has resulted from second-order random wave theory. We seek then to identify a consistent first-order history, $x_1(t)$, whose induced second-order correction, $x_2(t)$, satisfies $x_1(t) + x_2(t)$=$x_{obs}(t)$. Equivalently, we seek first-order Fourier coefficients $X_{1,k}$ such that $X_{1,k} + X_{2,k}$=$X_{o,k}$ (to within a prescribed tolerance). Once found, spatial extrapolation of $x_{obs}(t)$ to other locations follows by applying linear dispersion "selectively"—i.e., to $x_1(t)$ only—after which second-order corrections are calculated at each new location.

To identify $x_1(t)$ by an optimization procedure, it is convenient to separate real and imaginary components into separate vectors:

$$\mathbf{A} = \left[\frac{\mathrm{Re}\mathbf{X_1}}{\mathrm{Im}\mathbf{X_1}}\right] = \left[\frac{\mathbf{U}}{\mathbf{V}}\right] \; ; \quad \mathbf{B} = \left[\frac{\mathrm{Re}\mathbf{X_2}}{\mathrm{Im}\mathbf{X_2}}\right] \; ; \quad \mathbf{C} = \left[\frac{\mathrm{Re}\mathbf{X_o}}{\mathrm{Im}\mathbf{X_o}}\right] \tag{4}$$

Note that the vector $\mathbf{A}$, of length N, includes the real parts of $X_{1,k};\ k = 1 \ldots N/2$ and the imaginary parts of $X_{1,k};\ k = 1 \ldots N/2$. Similarly, $\mathbf{B}$ and $\mathbf{C}$, each of length N, contain real and imaginary parts of the lower half of $X_{2,k}$ and $X_{o,k}$, respectively.

Our goal here is to identify $\mathbf{A}$—and hence the digitized history $x_1(t)$—for which the length of the vector function

$$\mathbf{f}(\mathbf{A}) = \mathbf{A} + \mathbf{B} - \mathbf{C} \tag{5}$$

is minimized (ideally, set to zero). If $\mathbf{A}^{(p)}$ is an estimate of $\mathbf{A}$ at iteration p, $\mathbf{f}(\mathbf{A})$ can be linearized around $\mathbf{A}^{(p)}$ as

$$\mathbf{f}\left(\mathbf{A}\right) = \mathbf{f}\left(\mathbf{A}^{(p)}\right) + [J]\left(\mathbf{A} - \mathbf{A}^{(p)}\right) \tag{6}$$

where $[J]$ is a $N \times N$ Jacobian matrix containing the derivatives of the elements f_k in vector $\mathbf{f}(\mathbf{A})$ with respect to each of the unknowns a_l in $\mathbf{A}$ where $k, l = 1 \ldots N$. Setting $\mathbf{f}\left(\mathbf{A}\right)$=0 in Eq. 6, the Newton-Raphson scheme at iteration $p+1$ yields the updated estimate

$$\mathbf{A}^{(p+1)} = \mathbf{A}^{(p)} + \mathbf{h} \; ; \quad [J]\,\mathbf{h} = -\mathbf{f}\left(\mathbf{A}^{(p)}\right) \tag{7}$$

This Newton-Raphson iteration has been implemented (Sweetman and Winterstein, 1998), and found useful in identifying first-order histories consistent with various observed histories. Note that it involves simultaneous optimization of N unknowns; specifically, the real and imaginary parts of the below-Nyquist frequency Fourier components of $x_1(t)$. (Recall, for example, that N=24000 in the foregoing, realistic example.) While computationally intensive for large N, the algorithm has remained feasible for several reasons: (1) because its cost grows nonlinearly with N, identification is commonly applied first to various portions of the total history, and the results concatenated; and (2) the gradients of the Jacobian matrix in Eqs. 6–7 are available analytically (Appendix A).

Numerical Results

To illustrate these concepts, 10 simulations of the total wave elevation $x(t)$ have been found from second-order theory (Eqs. 1–3). We again assign a JONSWAP spectral model with

parameters H_S=15.4m, T_P=17.8s, and γ=1.7. It is useful to associate T_P with a corresponding wave length L_P=g/2πT_p^2=494m, and resulting steepness S_P=H_S/L_P=0.031. Assuming each of these simulations are "observed" at location Δ=0, we use three approaches to predict "consistent" wave histories at locations Δ=100–500m (i.e., up to roughly L_P, a characteristic wave length):

- Linear dispersion applied to $x(t)$
- Linear dispersion applied to $x(t)$, supplemented by a second-order contribution at each new location.
- Selective linear dispersion, which is applied to only the identified first-order process $x_1(t)$ corresponding to $x(t)$. This results in corresponding first-order processes at the other locations. Finally, consistent second-order contributions are added at each location.

We may expect that linear dispersion, while consistent with second-order wave theory, will by its linear nature tend to Gaussianize the wave process. Our selective linear dispersion addresses this by applying this linear operation to only the Gaussian part of $x(t)$.

Figures 3–5 show average results across the 10 simulations for the standard deviation, σ, skewness, α_3, and kurtosis, α_4, of the predicted wave histories. These figures also show exact moment results, which may be found from second-order theory (e.g., Jha and Winterstein, 2000):

$$\sigma = H_S/4 = 3.85\text{m} \;;\quad \alpha_3 = 5.45\gamma^{-0.084}S_p = 0.162\,;\quad \alpha_4 = 3 + 1.41\alpha_3^2\gamma^{0.02} = 3.07 \quad (8)$$

Our new, selective linear dispersion method is shown to most accurately follow each of these wave moments. As anticipated, linear dispersion tends to Gaussianize the wave, most notably by driving the skewness effectively to zero. Adding a second-order contribution to this linear dispersion result enhances non-Gaussian effects such as skewness; however, the standard deviation is overpredicted due to the double-counting of second-order effects. Finally, Figure 6 shows the average 3-hour maxima from each of the prediction methods. While there are no exact results here for confirmation, the preceding moment comparisons suggest that selective linear dispersion yields the most spatially consistent results. In comparison, simple linear dispersion underestimates maxima (due to its lack of skewness), while linear dispersion with second-order additions somewhat overestimates maxima (likely due to its larger standard deviation).

Summary and Conclusions

A new method has been shown here to identify Gaussian and non-Gaussian contributions from an observed wave history. This method yields a first-order history $x_1(t)$ which, when combined with corrections $x_2(t)$ from second-order wave theory, provides a total history that matches the observed record at each time point. Formally, a Newton-Raphson iteration is performed to simultaneously optimize the N unknown Fourier coefficients of $x_1(t)$ (Eqs. 4–7).

The value of this identification method is demonstrated here in cases where wave histories must be extrapolated spatially—e.g., for spatially distributed ocean structures and ships. The standard linear dispersion approach, while consistent with second-order theory, is shown to produce unstable spatial wave statistics, producing more nearly Gaussian behavior after spatial extrapolation. In contrast, the identification method proposed here permits "selective linear dispersion," applied only to the identified Gaussian part of the total wave process. This selective linear dispersion is found to yield spatially stable non-Gaussian models, accurately preserving the theoretical statistics of second-order random waves.

Acknowledgements

Portions of this work have been funded by the Office of Naval Research (Dr. Roshdy Barsoum, Program Manager) and by the industry sponsors of the Reliability of Marine Structures Program of Stanford University.

Appendix A: Explicit Form of Jacobian Matrix

It can be easily shown from Eqs. 4–5 that the Jacobian matrix $J_{k,l}$ is of the form

$$[J] = [I] + \left[\begin{array}{c|c} \dfrac{\partial \mathrm{Re}X_{2,k}}{\partial U_l} & \dfrac{\partial \mathrm{Re}X_{2,k}}{\partial V_l} \\ \hline \dfrac{\partial \mathrm{Im}X_{2,k}}{\partial U_l} & \dfrac{\partial \mathrm{Im}X_{2,k}}{\partial V_l} \end{array}\right] \tag{9}$$

where $[I]$ is the identity matrix, and the remaining terms follow from Eqs. 2–3:

$$\begin{aligned}
\frac{\partial \mathrm{Re}X_{2,k}}{\partial U_l} &= \sum_{m+n,k} (U_n\delta_{ml} + U_m\delta_{nl})\, H^+_{mn} + \sum_{m-n,k} (U_n\delta_{ml} + U_m\delta_{nl})\, H^-_{mn} \\
\frac{\partial \mathrm{Re}X_{2,k}}{\partial V_l} &= \sum_{m+n,k} -(V_n\delta_{ml} + V_m\delta_{nl})\, H^+_{mn} + \sum_{m-n,k} (V_n\delta_{ml} + V_m\delta_{nl})\, H^-_{mn} \\
\frac{\partial \mathrm{Im}X_{2,k}}{\partial U_l} &= \sum_{m+n,k} (V_m\delta_{nl} + V_n\delta_{ml})\, H^+_{mn} + \sum_{m-n,k} (V_m\delta_{nl} - V_n\delta_{ml})\, H^-_{mn} \\
\frac{\partial \mathrm{Im}X_{2,k}}{\partial V_l} &= \sum_{m+n,k} (U_n\delta_{ml} + U_m\delta_{nl})\, H^+_{mn} + \sum_{m-n,k} (U_n\delta_{ml} - U_m\delta_{nl})\, H^-_{mn}
\end{aligned} \tag{10}$$

References

Hasselmann, K. (1962). On the non-linear energy transfer in a gravity-wave spectrum. *J. Fluid Mech.*, 481–500.

Jha, A.K. and S.R. Winterstein (1997). *Nonlinear random ocean waves: prediction and comparison with data*, Rept. RMS–24, Reliability of Marine Structures Program, Dept. of Civ. Eng., Stanford University.

Jha, A.K. and S.R. Winterstein (2000). Nonlinear random ocean waves: prediction and comparison with data. *Proc., 19th Intl. Offshore Mech. Arctic Eng. Symp.*, ASME, Paper No. OMAE 00–6125.

Sweetman, B. and S.R. Winterstein (1998). *Second-order random ocean waves: prediction of temporal and spatial variation from fixed and moving references: the WAVEMAKER routine (Ver. 3.2)*, Rept. RMS–37, Reliability of Marine Structures Program, Dept. of Civ. & Environ. Eng., Stanford University.

Tick, L.J. (1959). A non-linear random model of gravitry waves I. *J. Math. & Mech.*, **8**(5), 643–651.

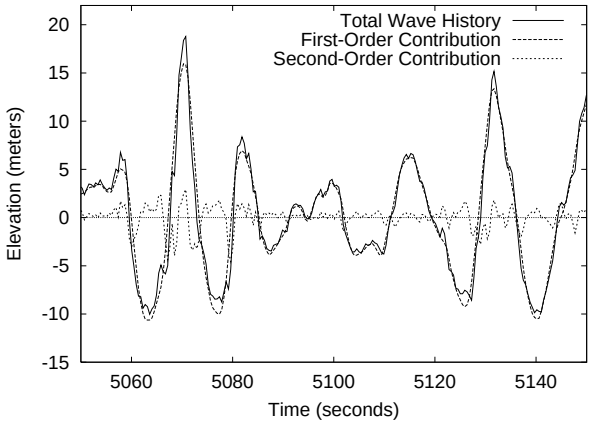

Figure 1: Time Histories.

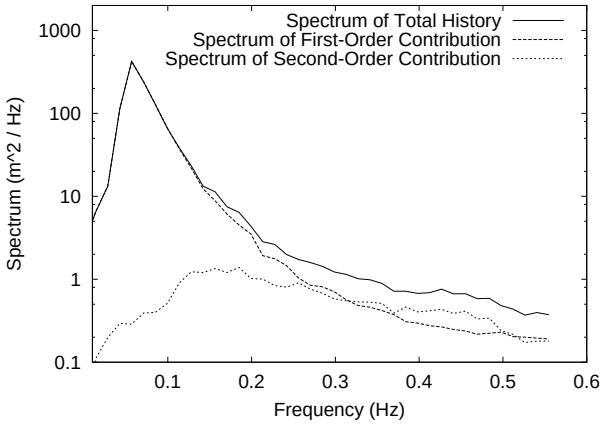

Figure 2: Power Spectra.

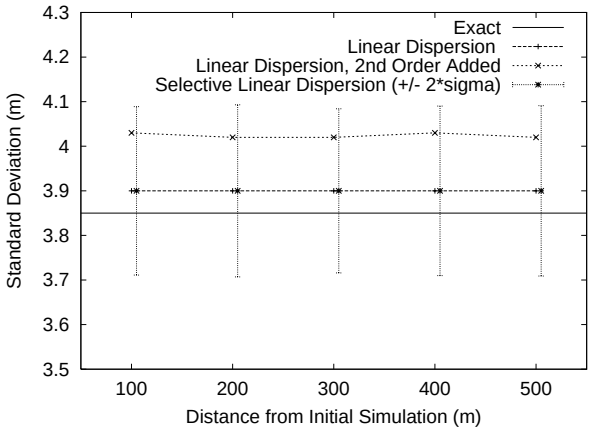

Figure 3: Standard Deviations.

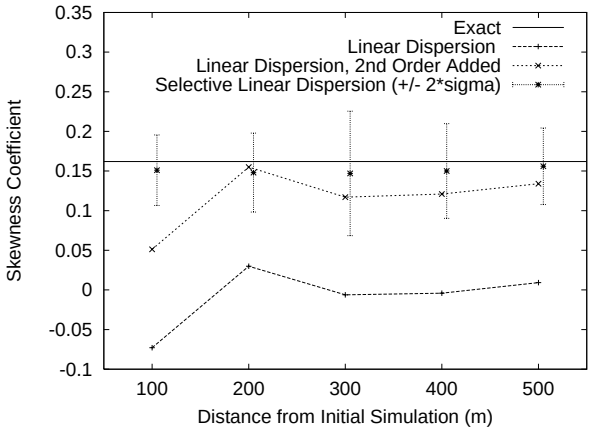

Figure 4: Skewness Coefficients.

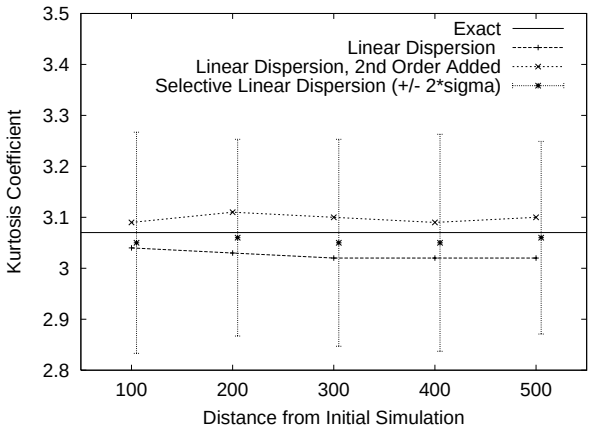

Figure 5: Kurtosis Coefficients.

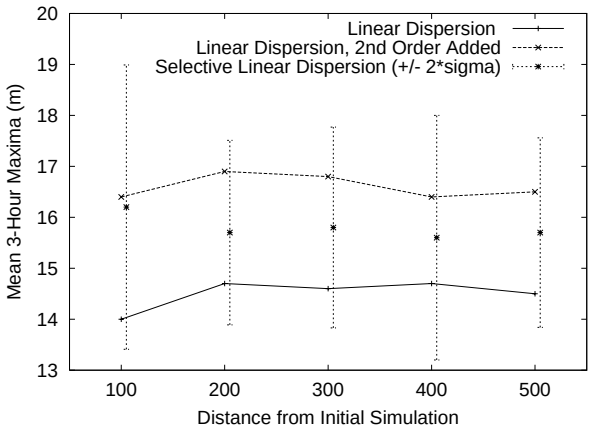

Figure 6: Mean 3-Hour Maxima.

Wave Statistics Across 500m Spatial Extrapolation; Various Methods

H_s=15.4 meters, T_p=17.8 seconds